Supporting Information

Michael *et al*. 10.1073/pnas.0802128105

SI Text

ES Cells. Phage clones spanning exon1α of PKG1α were isolated from a mouse 129 genomic library (Stratagene) and used to construct a targeting vector according to standard procedures. Along with the mutant exon 1α sequence containing point mutations in codons 12, 19, 26, and 33, an additional silent mutation was incorporated as a single base substitution at +15 in the coding sequence to introduce a XhoI restriction site, tagging the mutant exon. The targeting vector contained 9 kb of homology to the genomic locus, and incorporated a self-editing, LoxP flanked protamine Cre-POLII-*Neomycin* cassette. After electroporation, 1,000 G418-resistant clones were analyzed by Southern blot hybridization using an external probe to detect a diagnostic EcoRI polymorphism in the targeted locus. Mutations were sequentially introduced with a PCR based site-directed mutagenesis strategy (QuikChange; Stratagene) using a subcloned restriction fragment as substrate. All PCR product incorporated in the final targeting vector was verified by bi-directional sequencing. Conditions for growth and electroporation of CCE embryonic stem cells, G418 selection and preparation of chimeric mice were as described (1). Three targeted clones were identified in the first screen, but only two of these had incorporated the mutant exon sequence, and germline chimeras were created from one of these. The absence of an 8.8-kb BglII hybridizing fragment that is present in the chimera and targeted ES cell line shows that protamine Cre-mediated excision of the cassette successfully occurred in all heterozygous offspring, restoring the allele to the WT size of 4.8 kb (Fig. S1 *B* and *C*). An XhoI digest confirms the presence of the 3.8-kb mutant exon polymorphism in the targeted ES cell line and is retained in all seven heterozygous mice (Fig. S1*C*).

Animal Care and Naming. Throughout the studies described herein, animal care was in accordance with and approved by the Institutional Animal Care and Use Committee of Tufts University School of Medicine. The first LZM mouse line created is referred to as the "original" LZM colony and all studies in the MS are done with these unless otherwise noted. Two additional mouse LZM lines were created in 2005–2006 by introduction of targeted SV129 ES cells into both C57Bl6 blastocysts (LZM06 C57Bl6) and SV129 blastocysts (LZM06 SV129). These two lines were used to evaluate the reproducibility of the heritable blood pressure phenotype in multiple mouse lines, as described in the manuscript.

RT-PCR. Lung tissues from genotyped mice were flash frozen in liquid nitrogen, ground to powder with pestle and mortar, and RNA extracted with TRIzol (Invitrogen) as described by the manufacturer. One to 2 μg of total RNA and primers homologous to PKGI exon 2 sequence (+349) were subjected to RT reactions using SuperScript reverse transcriptase as recommended by the manufacturer (Invitrogen). Exon 1 upstream primer (+13) was then added and PCR performed using the Platinum (hot start) PCR mix. Product was digested with EarI and analyzed by 1.5% agarose gel electrophoresis (Fig. S2).

Purification of GST Fusion Proteins. GST-fusion proteins were expressed in E.coli XL10-gold (Stratagene) and purified on glutathione-agarose beads as described (2). Purified GST-fusion proteins were quantified by the Micro BCA Protein Assay Reagent Kit (Pierce) and analyzed by SDS/PAGE. GST-fusions used in these studies include the amino-terminal 59 aa of PKG1α and LZMPKG1α, the amino-terminal 70 aa of PKG1β, and the carboxy-terminal 100 aa of the myosin binding subunit (MBS) of MLCP.

Immunoblotting and GST Pull-Down Experiments. Experiments were performed as described (2–4). For immunoblotting, antibodies were raised against GST-peptides corresponding to WT or LZM PKG N-terminal 59 aa as described (3, 4). Commercial antibodies used in these studies include; RhoA (polyclonal, Santa Cruz Biotechnology), RhoA-S188-PO4 (Stressgen), myosin binding subunit of MLCP (MYPT1, Covance), myosin heavy chain (monoclonal, Sigma), α-actin (monoclonal, Sigma), smoothelin (polyclonal, Santa Cruz Biotechnology), calponin (monoclonal, Calbiochem), PKGII (polyclonal, Santa Cruz Biotechnology) and PKGcomm (cGPK1; Stressgen). Protein lysates were produced from lung tissue by flash freezing in liquid nitrogen and grinding to a powder with a pestle and mortar. Lysis buffer (50 mM Tris·HCl, pH 7.5, 7 mM $MgCl_2$, 2 mM EDTA, 2 mg/ml *n*-dodecyl-B-maltoside, 0.4 mg/ml cholesteryl hemisuccinate, 0.6 M NaCl, 10 mM Na Molybdate, 1 mM PMSF, 10 μg/ml chymostatin, 200 μg/ml aprotinin, 50 μg/ml leupeptin) was added and tissue was further homogenized with the pestle. After incubation on ice for 1 h, the sample was spun at top speed in the microcentrifuge for 20 min at 4°C. Protein lysates were made from WT and LZM VSMCs in culture as described (5). Protein in the supernatants was quantified using the BCA-200 kit (Pierce); 20-μg aliquots were resolved by polyacrylamide gel electrophoresis using Nupage 4–12% gradient gels (Invitrogen) followed by electrotransfer to Protran nitrocellulose. The membrane was blocked with PBS containing 0.05% Tween and 5% milk powder. Primary antibody incubation (1 h) in blocking solution was followed by washing (3 × 5 min) and addition of the secondary horseradish peroxidase conjugated anti-rabbit IgG (1:500 dilution; Amersham Life Science) in blocking solution (1 h). After washing, membranes were developed on film using ECL (Amersham). For densitometric analysis, immunoblotted bands were quantitated using an Alpha Innotech image analyzer and the data were plotted using SigmaPlot.

RhoA Activity and RhoA-S188-PO_4. RhoA activation and RhoA-S188-PO_4 assays were performed on serum-deprived WT and LZM VSMCs. For RhoA activation, GTP-bound RhoA was measured using GST-Rhotekin-RBD binding assays as described (5). For determination of RhoA-S188-PO_4, WT and LZM VSMC lysates were resolved by SDS/PAGE and immunoblotted with anti-RhoA-S188-PO_4 antibodies as described above.

PKGI Kinase Assay. VSMCs from PKG-LZM mice or WT littermates were rinsed in PBS, then lysed in PEM buffer (0.1 mM phenylmethylsulfonyl fluoride, 2 mM EDTA, 15 mM 2-mercaptoethanol, and 20 mM KH_2PO_4, pH 6.8) containing protease inhibitors (0.01 μg/ml each of aprotinin, leupeptin, and pepstatin A). The cell suspension was homogenized with a 26-gauge needle, and centrifuged at 10,000 × *g* for 10 min. The supernatant was used to measure PKG activities. The PKG activities were determined by measuring the transfer of [γ-^{32}P] phosphoryl group of ATP to BPDEtide (RKISASEFDRPLR from BIOMOL Research Laboratories), a specific substrate for PKG (6). Twenty micrograms of VSMC lysates was added to 50 μl of a reaction mixture containing 50 mM Tris buffer (pH 7.4), 5 mM magnesium acetate, 10 nM calyculinA, and 100 μM BPDEtide, with or without 10 μM 8-Br-cGMP. The reaction was initiated

by adding 10 μCi of [γ-^{32}P]ATP and was incubated for 20 min at 30°C. The reaction was terminated by spotting 50 μl of the reaction mixture onto Whatman P-81 phosphocellulose paper. After six washes in 75 mM phosphoric acid and two ethanol rinses, the papers were dried, then added to a scintillation vial containing 5 ml of scintillant and PKG activity was determined by Cerenkov counting. Samples of each lysate were analyzed for PKG quantity by SDS/PAGE and immunoblotting, and these values were used to normalize the PKG activity.

PKG-II Expression in the Kidneys in WT and LZM Mice. Bilateral kidneys were taken from four WT and four LZM male mice (all 4 months old). The kidneys were weighed, homogenized, dissolved in lysis buffer (see above), passed through a 25-gauge needle and centrifuged at 15,000 rpm for 20 min. After adjusting the total protein concentration so that all of the samples had equivalent protein loading, 1 ml of supernatant was mixed with rabbit polyclonal anti-PKG-II antibodies and rocked overnight. Protein-G beads were then added and the samples were incubated for 2 h. The beads were pelleted, washed four times in lysis buffer and then mixed with SDS-sample buffer. The samples were electrophoresed on 6% SDS/PAGE gels and immunoblotted with the same anti-PKG-II antibodies.

Electrophysiological Recordings from WT and LZM VSMC. ***Isolation of single smooth muscle cells from cerebral arteries.*** Cerebral (basilar) arteries from WT and LZM mice were digested in 0.3 mg/ml papain and 1 mg/ml dithioerythritol for 10 min, and then transferred for a second digestion in 1 mg/ml collagenase (type F and type H in a 70%–30% mixture, respectively) for 7 min. The digested tissue was triturated with a fire polished glass Pasteur pipette to yield single smooth muscle cells (7).

Patch clamp recordings. Isolated myocytes from cerebral arteries were bathed in physiological salt solution (134 mM NaCl, 6 mM KCl, 1 mM MgCl2, 2 mM CaCl2, 10 mM glucose, 10 mM Hepes pH 7.4). Whole cell potassium currents were recorded in response to voltage steps from −80 mV to +80 mV in 20 mV steps (pulse duration, 250 ms) (20–22°C), using the whole cell perforated patch technique (7). The pipette solution contained 110 mM K-aspartate, 30 mM KCl, 10 mM NaCl, 1 mM $MgCl_2$, 10 mM Hepes (pH 7.2), and 250 mg/ml amphotericin B. Currents were filtered at 1 kHz and digitized at 4 kHz.

***In Vivo* Stress Fiber Staining.** Four WT and four LZM mice, all 4 months old, were anesthetized and then perfused systemically with 4% formaldehyde in isotonic saline (pH 7.4) for 5 min. The aortas were resected and further fixed in the same perfusion solution for 20 min, and the endothelium was denuded. Actin contractile stress fibers were labeled as described (8).

VSMC Morphology and Immunofluorescence. VSMCs cultured on gelatin coated glass coverslips were fixed with 3.7% paraformaldehyde, permeabilized with 0.3% Triton X, blocked with 10% donkey serum and incubated with Alexa 488 or 568 phalloidin (Molecular Probes) and primary antibodies (anti-RhoA, Santa Cruz Biotechnology, anti-RhoA-S188-PO4, Stressgen) for 1 h. After three rinses with PBS, secondary antibody conjugated with Cy3 (Jackson ImmunoResearch) was added and incubated for one hour. The coverslips were washed three times in PBS and mounted on slides with Slowfade reagent (Molecular Probes) for analysis with a Nikon Optiphot-2 fluorescence microscope and a Spot charge coupled device camera (Diagnostic Instruments). Stress fibers were manually counted in WT ($n = 17$) and LZM ($n = 15$) VSMCs after phalloidin labeling. Cell surface area was calculated by an investigator blinded to the mouse genotype using computerized morphometric software (Image Pro 4.1, Media Cybernetics). Explant and enzymatic preparations of primary, unpassaged VSMC were made as described previously (9).

Murine Vascular Ring Studies. Vascular ring studies were performed with mouse thoracic aortas. Aortic rings were prepared, equilibrated and mounted on force transducers in bioassay chambers as described previously (3, 10). Contractile responses to KCL and phenylephrine were performed in all vascular ring assays. There was no difference between WT (0.165 ± 0.01 g) and PKGI-LZM KI (0.121 ± 0.01 g) mice ($n = 12$ each) in response to KCL (30 mM) and to phenylephrine in the dose range of 10^{-8} M to 3×10^{-6} M (data not shown). Following maximal contraction with phenylephrine (PE, vertical arrow), increasing concentrations of either Ach or 8Br-cGMP were applied. In all studies with endothelium-intact rings, the integrity of the endothelium was confirmed by demonstrating relaxation to acetylcholine before any further experimentation, as described (3, 10). Similarly, endothelial-denuded rings were routinely checked for unresponsiveness to acetylcholine following denudation before further study. Eight chambers were analyzed simultaneously (four WT, four LZM). For Ach relaxation, total rings studied: WT, $n = 19$; LZM, $n = 29$. For 8Br-cGMP studies, $n = 6$ rings were studied.

Isolated Resistance Arterial Preparation. All animals were killed with an overdose of pentobarbital solution (200 mg/kg i.p.) in accordance with institutional guide lines and approved by the Institutional Animal Care and Use Committee of the University of Vermont. After animals were killed, the brain was removed and placed into oxygenated ice-cold artificial cerebrospinal fluid (PSS, for composition see below). Posterior cerebral arteries were isolated and dissected from the surrounding connective tissue. Arteries were then cannulated, and mounted in a specially designed close working distance arteriograph. Experiments with intact arteries were done under continuous superfusion with PSS at 37°C, gassed (95% O_2/5% CO_2), and PSS solution was used with the following constituents: 119 mM NaCl, 4.7 mM KCl, 24 mM $NaHCO_3$, 1.2 mM KH_2PO_4, 0.0023 mM EDTA, 1.2 mM $MgCl_2$, 11 mM glucose, and 2.5 mM $CaCl_2$ (pH 7.4). Only arteries that constricted to pressure were used. Arterial diameters were measured with a video dimension analyzer (Ionoptix).

The development of tone in response to elevating pressure to 80 mmHg and application of LNNA is expressed as the percent constriction relative to maximal diameter, calculated as: Constriction (%) = (IDmax − IDS)/IDmax × 100. IDmax is the maximal inner diameter recorded at a pressure of 80 mmHg and IDS is the steady-state diameter measured subsequent to each incremental change in stimulus. Dilatory responses to application of sodium nitroprusside are expressed as percent dilation relative to starting baseline diameter and maximal diameter, calculated as: Dilation (%) = (IDS − IDB)/(IDmax − IDB) × 100. IDB is the starting baseline diameter. Maximal diameter at given intravascular pressure was determined by applying calcium-free PSS with 5 mM EGTA and 100 μM papaverine.

Telemetric Blood Pressure Measurements. Telemetric blood pressure measurements were made in ambulatory mice using implantable, miniaturized mouse blood pressure transmitters (Data Sciences International) as described (3, 10). Transducer sampling frequency was hourly at 500 hfr/sec for five seconds (2,500 points per hour). All animal procedures and experiments were approved by the Tufts Medical Center institutional animal use and care committee. Aldosterone levels were measured by commercial RIA (Diagnostic Labs).

Tail-Cuff Blood Pressure Measurements. Systolic, diastolic and mean blood pressures of conscious 6- to 12-month-old mice were measured using a tail cuff blood pressure analyzer designed with volume-pressure recording (VPR) technology (Model Coda6, Kent Scientific). Before measurement, animals were exposed to the environment and instrument on a daily basis for at least 7

days. All measurements were made with strict quiet and limited access to the room, which is designated solely for tail cuff blood pressure measurements in mice. Body temperature of the mice was maintained at above 37°C on a heated platform. The blood pressure of trained mice was monitored for 30–40 min and final values were obtained after 15 consecutive readings on each of two occasions during this period, whose values were within ± 5% of the mean. The mean value for each of these two sets of readings was then meaned and taken as the single blood pressure measurement for that animal and time point. Basal blood pressure was determined in mice fed with a normal diet containing 0.49% NaCl (Harlan Teklad). Mice were then switched to a high salt diet (high-salt chow = 6% NaCl, Harlan Teklad) allowed to equilibrate for 1 week on the diet, and then blood pressure was determined as above. The mice were then switched to a sodium deficient chow (Harlan Teklad) for 1 week, allowed to equilibrate, and then blood pressure was determined again as above. Mice were allowed free access to tap water at all times.

Renal Function Assays. Inulin clearance is used as a measure of glomerular filtration rate (GFR), and paraaminohippuric acid (PAH) clearance as an estimate of renal plasma flow (RPF). Clearances of inulin and PAH were measured as described by Coffman and coworkers (11, 12). Briefly, mice were anesthetized with 2.5% Isoflurane via nosecone and maintained at 37°C on a regulated heat pad. The ventral neck region was shaved and a 1.5 cm incision made from the chin to the clavicle and the left external jugular vein and left common carotid artery were bluntly then sharply dissected and isolated. The vein was cannulated with a 9 -inch length of PE10 attached to a 30G blunted needle and the artery cannulated with a 3inch length piece of PE10 but with a #2, 2.5-cm piece of silicone tubing connected to a 23-gauge needle to allow for clamping during arterial blood sampling. The bladder was exposed with a suprapubic incision and a 1-inch piece of PE50 with #2 silicone cuff inserted into a stab wound and circumferential tie securing the catheter in place. Normal saline was infused with a pump at 0.025 ml/min to deliver 1% of body weight over 20 min to replace surgical losses. Priming doses of [carboxyl-^{14}C]inulin and [glycyl-^{3}H]PAH were given, followed by infusion of [^{14}C]inulin, and [^{3}H]PAH in normal saline at a rate of 25 μl/min/100 g of body weight. After 30 min of equilibration, renal function was measured during three consecutive 30-min clearance periods. [^{14}C]Inulin and [^{3}H]PAH in plasma and urine were measured in a liquid scintillation counter (LS6500, Beckman Coulter), and clearances were calculated using standard formulas. Renal plasma flow for the WT and LZM mice were not different (WT vs. LZM = 31,785 ± 9,253 cpm vs. 33,927 ± 14,065 cpm, $P = 0.9$, $n = 3$).

Serum Chemistries and Complete Blood Counts. All measurements were performed by IDEXX Laboratories on serum obtaining by terminal exsanguination of WT and LZM mice.

Statistical Methods. All data are shown as mean ± SE except where noted as ± SD. For pairwise analysis, Student's *t* tests were used. Multiple group comparisons were made either by one-way ANOVA or two-way ANOVA, as appropriate. For significant between-group differences found by ANOVA, multiple pairwise comparisons were made with the Student–Newman–Keuls method. For all statistical comparisons, $P < 0.05$ was considered significant.

1. Michael SK, Brennan J, Robertson EJ (1999) Efficient gene-specific expression of Cre recombinase in the mouse embryo by targeted insertion of a novel IRES-Cre cassette into endogenous loci. *Mech Dev* 85:35–47.
2. Surks HK *et al.* (1999) Regulation of myosin phosphatase by a specific interaction with cGMP-dependent protein kinase Iα. *Science* 286:1583–1587.
3. Tang M, *et al*. (2003) Regulator of g-protein signaling 2 mediates vascular smooth muscle relaxation and blood pressure. *Nat Med* 9:1506–1512.
4. Surks HK, Richards CT, Mendelsohn ME (2003) Myosin phosphatase-Rho interacting protein: A new member of the myosin phosphatase complex that directly binds RhoA. *J Biol Chem* 278:51484–51493.
5. Surks HK, Riddick N, Ohtani K (2005) M-RIP targets myosin phosphatase to stress fibers to regulate myosin light chain phosphorylation in vascular smooth muscle cells. *J Biol Chem* 280:42543–42551.
6. Colbran JL, *et al*. (1992) A phenylalanine in peptide substrates provides for selectivity between cGMP- and cAMP-dependent protein kinases. *J Biol Chem* 267:9589–9594.
7. Brenner R, *et al*. (2000) Vasoregulation by the B1 subunit of the calcium-activated potassium channel. *Nature* 407:870–876.
8. Herman IM *et al*. (1987) Hemodynamics and the vascular endothelial cytoskeleton. *J Cell Biol* 105:291–302.
9. Karas RH, Patterson BL, Mendelsohn ME (1994) Human vascular smooth muscle cells contain functional estrogen receptor. *Circulation* 89:1943–1950.
10. Zhu Y, *et al*. (2002) Abnormal vascular function and hyptertension in mice deficient in estrogen receptor β. *Science* 295:505–508.
11. Spurney RF, Ruiz P, Pisetsky DS, Coffman TM (1991) Enhanced renal leukotriene production in murine lupus: role of lipoxygenase metabolites. *Kidney Int* 39:95–102.
12. Cervenka L, Mitchell KD, Oliverio MI, Coffman TM, Navar LG (1999) Renal function in the AT1A receptor knockout mouse during normal and volume-expanded conditions. *Kidney Int* 56:1855–1862.

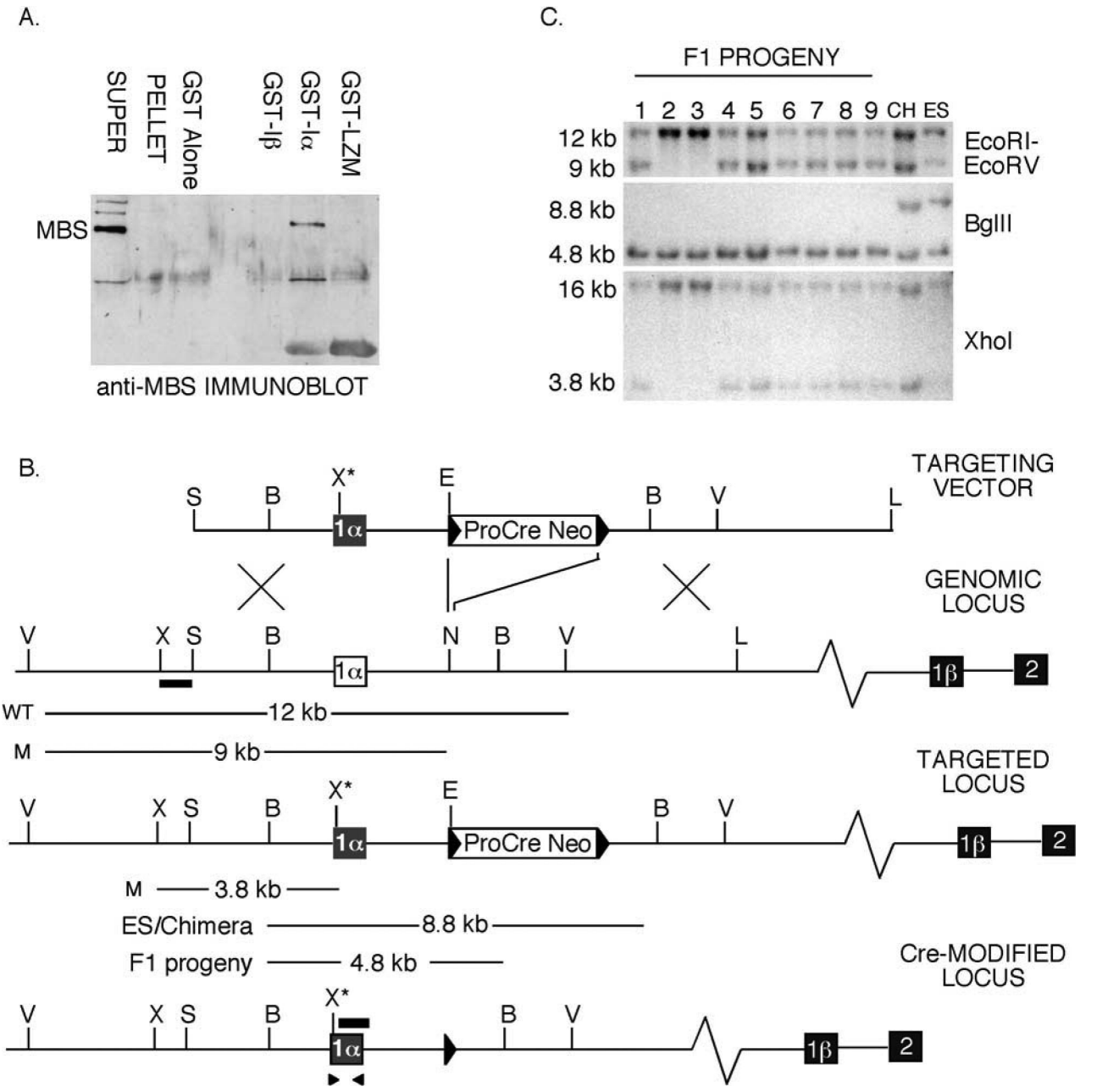

Fig. S1. Targeting of the mouse PKGIα locus. (*A*) $PKG_{1–59}$LZM fails to bind MBS, unlike native PKGIα LZ (control). WT and mutant PKGIα leucine zipper domain (LZ; amino acids 1–59) GST fusion proteins were incubated with VSMC lysates to confirm the loss of LZ-mediated PKGIα interaction with the myosin binding subunit (MBS) of myosin light chain phosphatase (further details, see ref. 2 and *SI Text*). (*B*) Generation of ES cells harboring the mutant PKGIα exon. Mice were genotyped by using primer pairs to region shown by small triangles under exon 1, followed by EarI digestion to distinguish genotypes. Large triangles denote LoxP sites. Small black rectangles indicate probes used in Southern blot analysis. S, SacI; N, NotI; X, XhoI; V, EcoRV; E, EcoRI; B, BglII; L, SalI; T, targeted. *, new site in mutant exon. (*C*) Southern blots showing restriction analysis of the targeted ES cell line, a chimera, and F_1 progeny. The presence of a 9-kb EcoRI polymorphism confirms germ-line transmission of the LZ mutant PKGIα allele in seven of nine offspring.

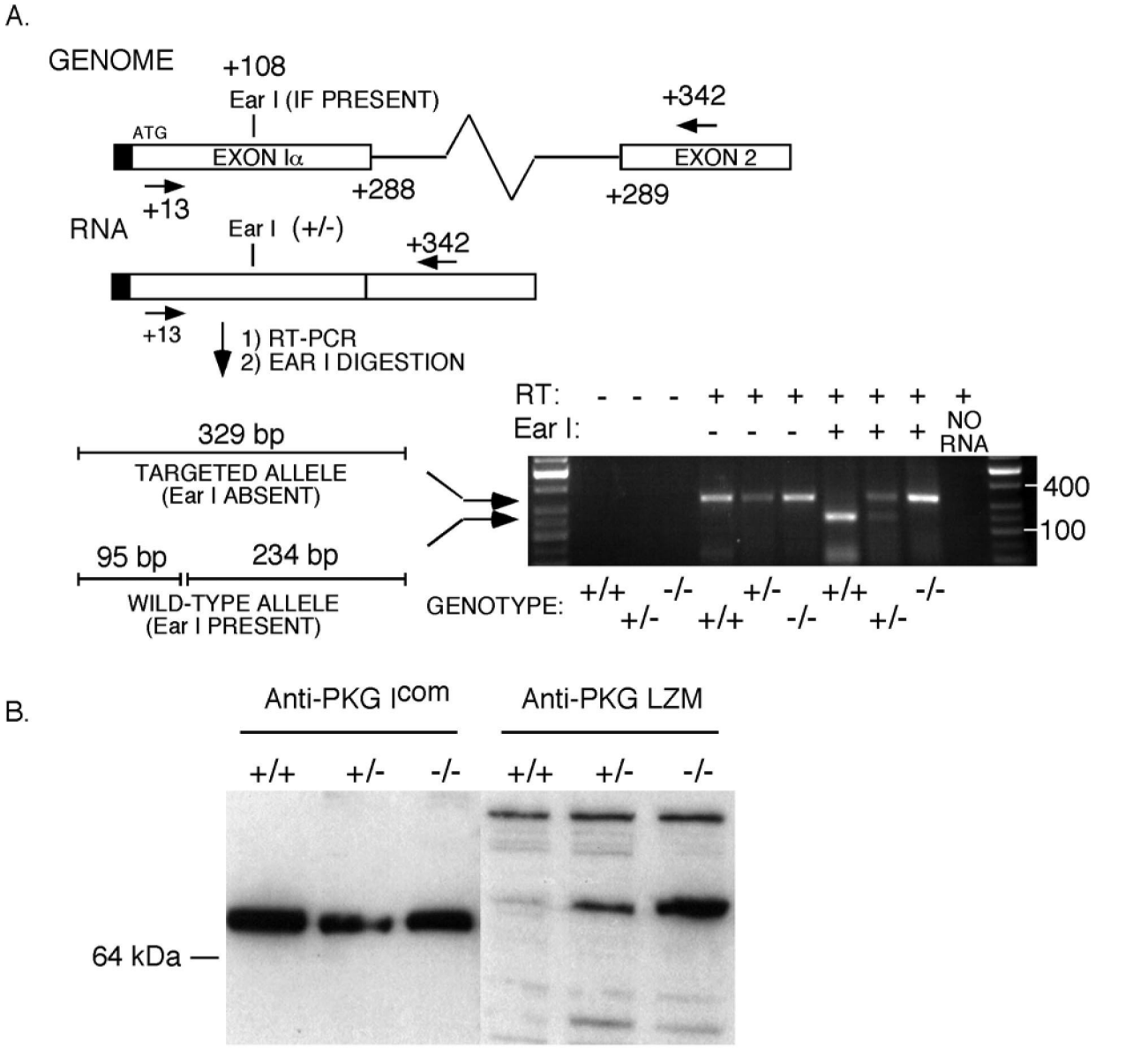

Fig. S2. Transcriptional and translational activity of the mutant of PKGIα allele. (*A*) RT-PCR to identify RNA transcript from LZ mutant ($-/-$), heterozygous ($+/-$) and WT ($+/+$) littermates. The PCR product of the LZM allele is distinguished by susceptibility to EarI digestion, which is absent in the WT allele. (*B*) Immunoblotting of lung lysates from the three genotypes with polyclonal anti-PKGIα antibody (PKGIcomm) or with an antibody raised to mutant PKGIα amino acid 1–59 LZ peptide (anti-PKG LZM).

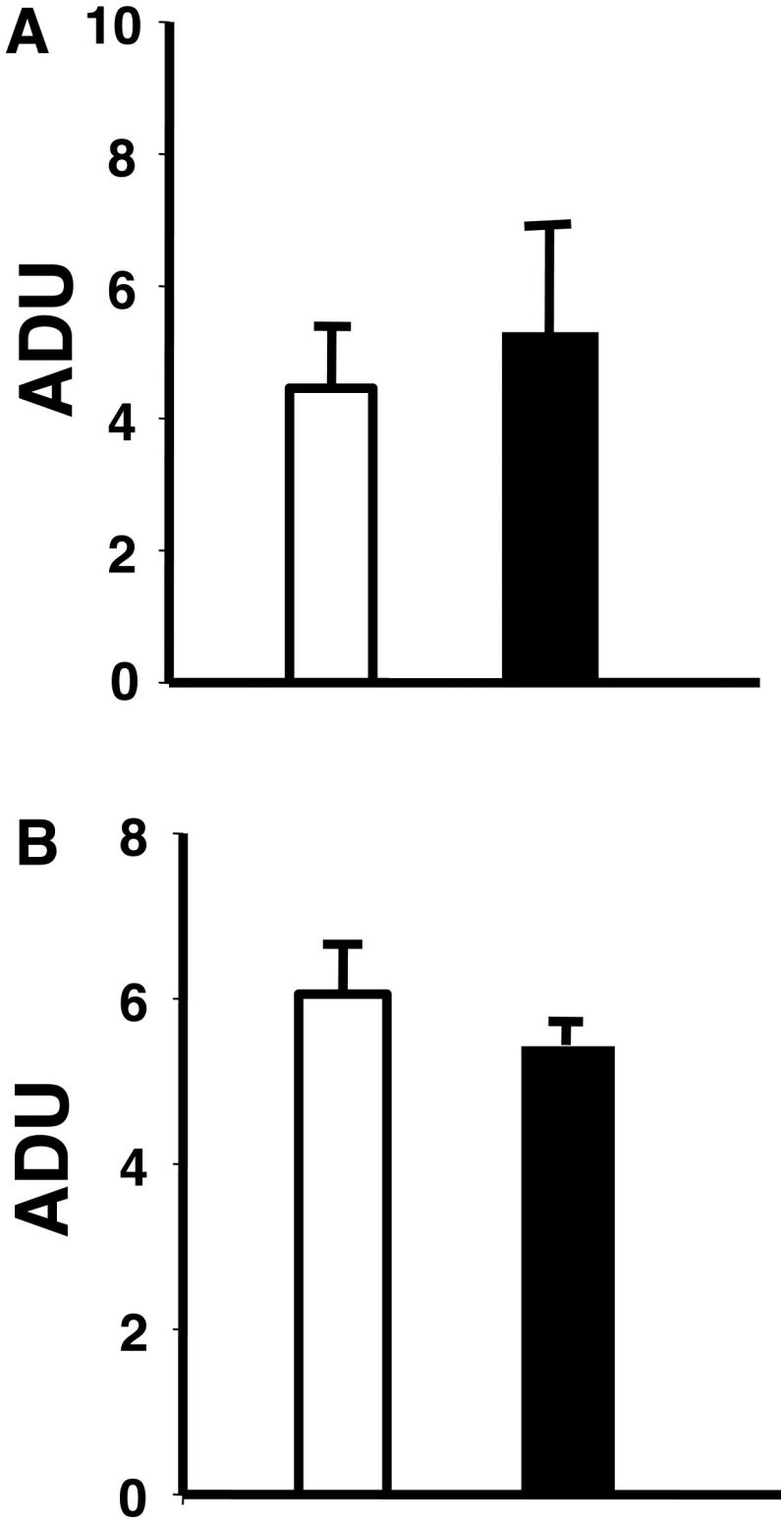

Fig. S3. Quantitative analysis of PKG expression in WT and LZM aortas. (*A*) Total PKG levels do not differ between WT and LZM aortas. Densitometric analysis of total PKG from WT and LZM aortas ($n = 3$, not statistically significant). (*B*) PKGIβ levels do not differ between WT and LZM aortas. Densitometric analysis of PKG1β from WT and LZM aortas ($n = 3$, not statistically significant). For *A* and *B*: white bar, WT; black bar, LZM.

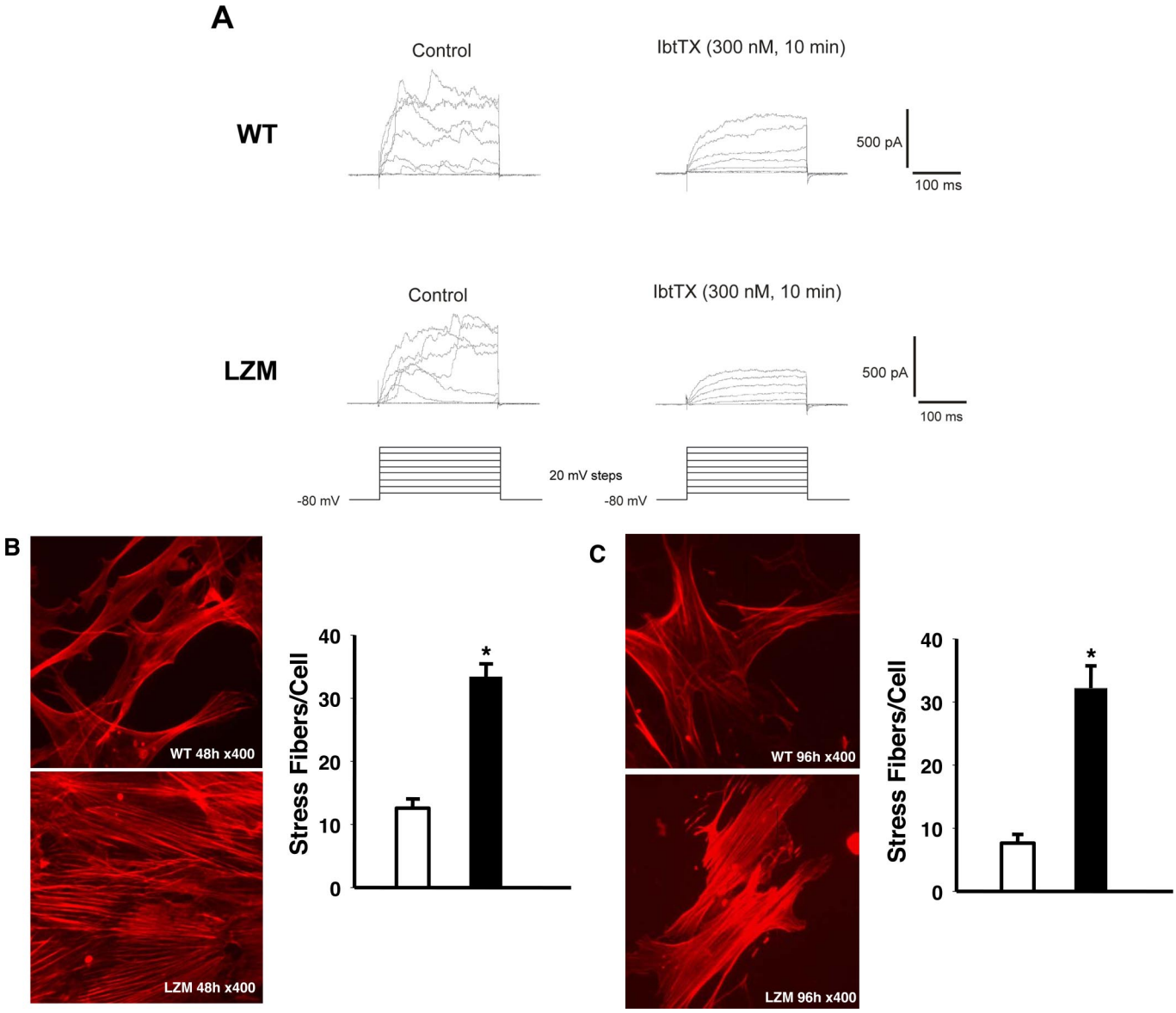

Fig. S4. Morphologic analysis of WT and LZM VSMCs. (*A*) Representative voltage-dependent potassium channel currents in cerebral artery myocytes from WT and LZM mice in the presence and absence of iberiotoxin. The current–voltage relationship of the whole-cell current was not different in the WT and LZM mice. At +40 mV, the peak outward currents in myocytes from WT and LZM mice were 486 ± 69 pA ($n = 5$) and 446 ± 130 pA ($n = 4$), respectively. (*B*) LZM VSMC derived by the explant method have significantly more stress fibers than WT cells. WT and LZM VSMC were immunofluorescently labeled with phalloidin to identify stress fibers 48 h after explant, and the number of stress fibers per cell were counted manually. Representative cells are shown in *Left*, and summary data from 20 cells per genotype are shown in *Right*. *, $P < 0.01$ vs. WT. White bar, WT; black bar, LZM. (*C*) LZM VSMC derived by enzymatic digestion of aortas have significantly more stress fibers than WT cells. WT and LZM VSMC 96 h after enzymatic digestion were immunofluorescently labeled with phalloidin to identify stress fibers, and the number of stress fibers per cell were counted manually. Representative cells are shown in *Left*, and summary data from 20 cells per genotype are shown in *Right*. *, $P < 0.01$ vs. WT. white bar, WT; black bar, LZM.

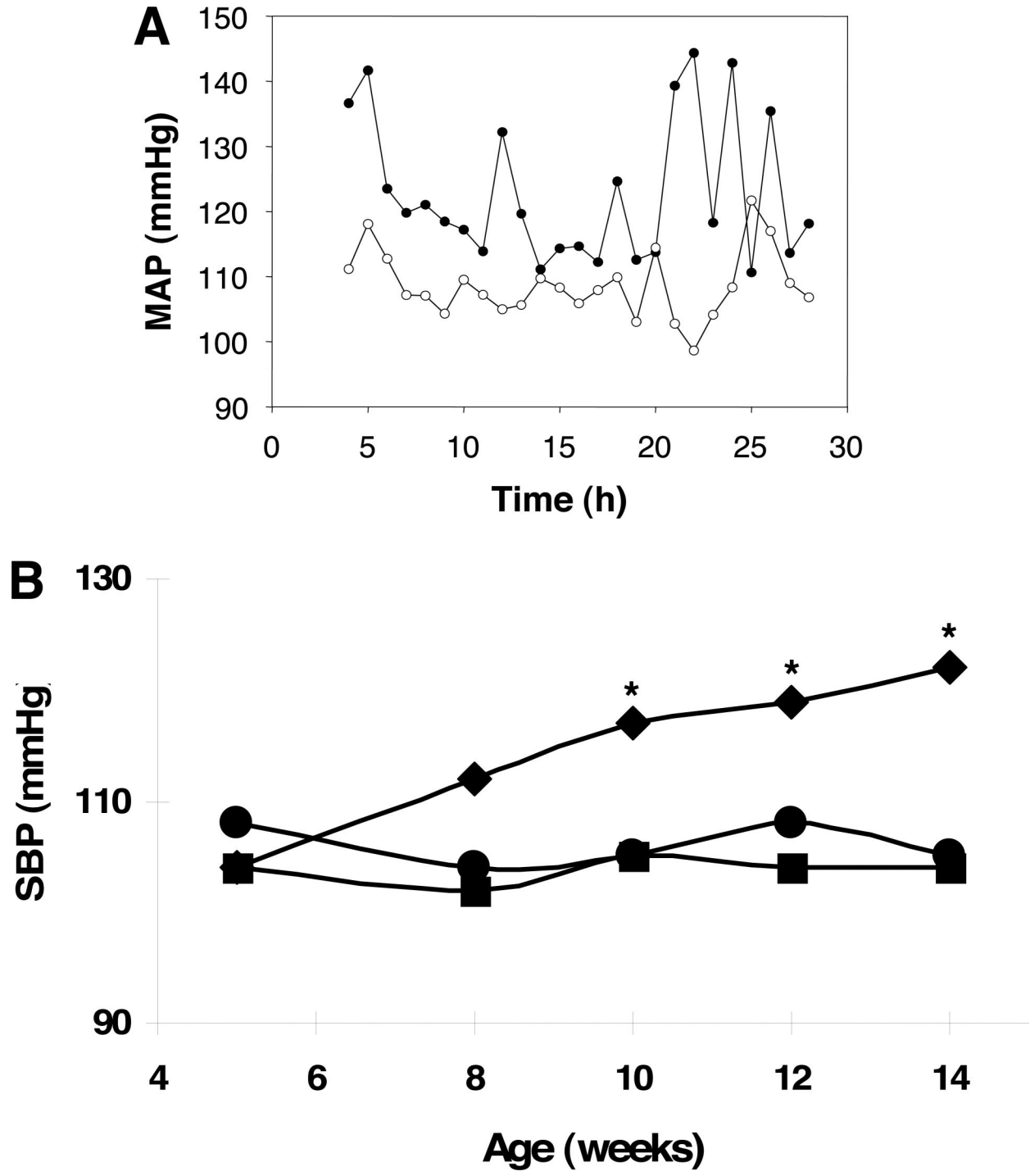

Fig. S5. Telemetry and tail cuff blood pressure time course measurements reveal hypertension in intact LZM mice. (*A*) Mean arterial pressure (MAP) recorded by in-dwelling telemetric blood pressure transducers in intact unanesthetized ambulatory mice. A 24-h cycle is shown for a representative LZM mouse compared to an age- and sex-matched WT littermate. (*B*) LZM mice develop hypertension at ≈10 weeks of age. Tail cuff blood pressure measurements of male WT (circles), heterozygous LZM (squares), and homozygous LZM (diamonds) mice were measured at weeks 5, 8, 10, 12, and 15. $n = 3$–4 mice per genotype; *, $P < 0.05$ vs. WT.

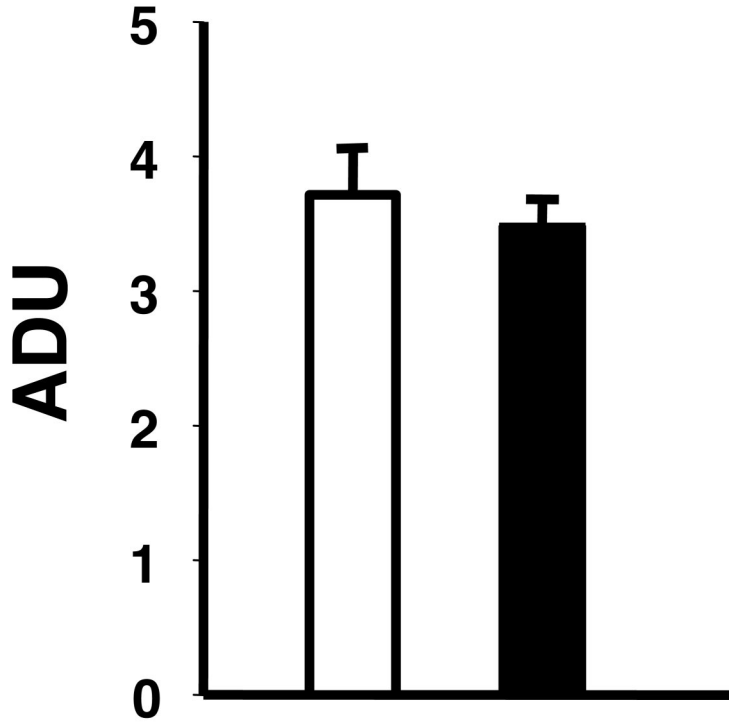

Fig. S6. PKGII is expressed at equivalent levels in the kidney of WT and LZM mice. PKGII expression was detected by immunoblotting of protein lysates of kidneys from WT and LZM mice. Densitometric analysis revealed no significant difference in renal PKGII abundance between WT and LZM mice (not statistically significant, $n = 4$). White bar, WT; black bar, LZM. ADU, arbitrary densitometric units.

Table S1. Body and organ weights of LZM and WT mice

	Weight, g	
Body/organ	LZM	WT
Body	44.4 ± 1.8	44.3 ± 3.8
Heart	0.16 ± 0.01	0.16 ± 0.01
Kidney	0.49 ± 0.01	0.53 ± 0.04
Liver	1.90 ± 0.11	1.78 ± 0.20
Lung	0.15 ± 0.01	0.16 ± 0.01

$n = 6$ for LZM-KI mice, and $n = 5$ for WT mice. Data are expressed as average ± SEM. Differences in all categories are not statistically significant.

Table S2. Telemetry blood pressures for male C57/BL6 (original) mice (n = 3–5 each genotype)

Pressure	WT	LZM	P value
Systolic, mmHg	117.8 ± 0.2	126.9 ± 0.2	<0.001
Diastolic, mmHg	93.9 ± 0.2	104.3 ± 1 mmHg	<0.001
MAP, mmHg	104.4 ± 0.1	114.4 ± 0.8	<0.001
Heart rate, beats/min	538 ± 3	544 ± 3	NS

Table S3. Tail cuff blood pressures for female LZM06 SV129 mice (n = 10 WT and 11 LZM)

Pressure	WT	LZM	P value
Systolic, mmHg	127 ± 2	140 ± 4	<0.05
Diastolic, mmHg	94 ± 3	105 ± 4	<0.05
MAP, mmHg	105 ± 3	116 ± 4	<0.05

(MAP, mean arterial pressure).

Table S4. Additional serum chemistries for LZM mice

	LZM	WT
Alkaline phosphatase, units/liter	59.7 ± 6.8	46.0 ± 4.8
SGPT (ALT), units/liter	32.8 ± 2.2	24.8 ± 2.4
SGOT (AST), units/liter	51.5 ± 1.8	38.0 ± 7.6
Total bilirubin, mg/dl	0.1	0.1
Direct bilirubin, mg/dl	0	0.1
Indirect bilirubin, mg/dl	0.1	0.0
Glucose, mg/dl	284.3 ± 18.6	284.4 ± 7.9
Cholesterol, mg/dl	159.2 ± 3.9	136.0 ± 4.6
CK, units/liter	51.5 ± 14.7	50.0 ± 22.8
Globulin, mg/dl	2.3 ± 0.1	2.1 ± 0.1

$n = 6$ for LZM-KI mice, and $n = 5$ for WT mice. Data are expressed as average ± SEM. Differences in all categories are not statistically significant.

Table S5. Complete blood counts for LZM and WT mice

	LZM	WT
WBC, thousands/μl	6.1 ± 0.6	8.7 ± 1.2
RBC, millions/μl	9.7 ± 0.3	8.8 ± 0.2
HGB, g/dl	14.3 ± 0.4	13.9 ± 0.2
HCT, %	56.3 ± 1.6	52.4 ± 1.0
MCV, fl	58 ± 0.7	60 ± 1.1
MCH, pg	14.8 ± 0.2	15.8 ± 0.4
MCHC, g/dl	25.6 ± 0.2	26.6 ± 0.5
NRBC, per 100 WBC	0.17 ± 0.17	0.00
Neutrophil seg, %	23 ± 2.7	22 ± 0.9
Neutrophil band, %	0.00	0.00
LYMPHOCYTE, %	73 ± 2.6	75 ± 1.4
MONOCYTE, %	2.5 ± 0.5	1.4 ± 0.2
EOSINOPHIL, %	1.3 ± 0.6	1.4 ± 0.5
BASOPHIL, %	0.00	0.00
Absolute neutrophil seg, per μl	1,446 ± 259	1,950 ± 259
Absolute neutrophil band, per μl	0.00	0.00
Absolute lymphocyte, per μl	4,436 ± 408	6,530 ± 900
Absolute monocyte, per μl	148 ± 30	117 ± 18
Absolute eosinophil, per μl	70 ± 34	122 ± 42
Absolute basophil, per μl	0.00	0.00

$n = 6$ for LZM-KI mice, and $n = 5$ for WT mice. Data are expressed as average ± SEM. Differences in all categories are not statistically significant.